Characteristics of flux pinning in $YBa_2Cu_3O_y/PrBa_2Cu_3O_y$ superlattices

H. C. Yang and L. M. Wang
Department of Physics, National Taiwan University, Taipei, Taiwan, Republic of China

H. E. Horng
Department of Physics, National Taiwan Normal University, Taipei, Taiwan, Republic of China

(Received 7 April 1998; revised manuscript received 7 August 1998)

The resistivity of $(YBa_2Cu_3O_y/PrBa_2Cu_3O_y)_n$ $[(YBCO/PBCO)_n]$ superlattices under magnetic fields was measured to investigate the flux pinning and anisotropic superconducting properties, where n is the number of the modulation layer. The fields applied were parallel to the *ab* plane and the *c* axis of the films. The resistivity under magnetic fields shows thermally activated behavior. A power law magnetic field dependence of $U_0 \sim H^{-\alpha}$ in YBCO/PBCO superlattices was observed. The $U_0 \times H^{\alpha}/(H_{c2,c})^2$ was observed to scale to a constant which increases linearly when the thickness of YBCO layers is increased and decreases linearly when the thickness of PBCO layers is increased. There exists both one-unit-cell YBCO and interlayer YBCO couplings in YBCO/PBCO superlattices. These couplings affect the coherence lengths. [S0163-1829(99)01010-3]

I. INTRODUCTION

Among the many remarkable mixed-state features of high-T_c superconductors, the mixed-state resistivity has attracted much attention.[1–3] The dc resistivity under magnetic field yields important information about the flux motion. For finite current density, the Lorentz force is sufficiently strong that the vortex lines in the vortex glass region can overcome a certain class of pinning barriers, leading to flux creep, and a finite voltage. Above the glass transition temperature. $T_g(H)$, the resistivity is nonzero and its temperature dependence, $\rho(T,H)=\rho_0 \exp(-U_0(T,H)/k_BT)$, follows an Arrehenius law; one has the thermally activated flux flow (TAFF).[3]

Regarding the flux pinning energy, theoretical work has suggested that the activation energy, $U_0(T,H)$, should depend logarithmically on the field[4] while experimental results have shown a power law dependence $U_0 \sim (1/H^{\alpha})$, for example, $\alpha=0.25-0.5$ for $Bi_2Sr_2CaCu_2O_8$.[3] Other works reported that U_0 cannot be fitted with a field dependence of the power law $U_0 \sim H^{-\alpha}$ for YBCO/PBCO superlattices in the whole investigated magnetic fields (up to 10 T).[5] An important question is to understand how the activation energy U_0 depends on the applied magnetic field in YBCO/PBCO superlattices in the thermally activated flux flow regime. We have chosen the YBCO/PBCO superlattices in this study because we can vary the pinning energy U_0 by varying the thickness of YBCO or PBCO layers. Besides, one can investigate the coupling between the YBCO layers or within the YBCO layers. In this work, in the pinning energy study we have observed a scaling behavior in $U_0 \sim H^{-\alpha}(H_{c2,c})^2$ for $(YBCO/PBCO)_n$ superlattices with different thickness of YBCO and PBCO layers, where U_0 is the pinning energy, H is the applied magnetic field, and $H_{c2,c}$ is the upper critical field with the applied field parallel to the *c* axis in the thermally activated flux flow regime. We also observed the coupling between one-unit-cell of YBCO layer and the interlayer YBCO coupling in YBCO/PBCO superlattices.

II. EXPERIMENTS

The $(YBCO/PBCO)_n$ superlattices were prepared by the rf magnetron sputtering techniques. A detailed description of the growth and characterization of YBCO/PBCO superlattices has been reported in Refs. 6 and 7. In resistivity measurements the film was patterned to a resistivity geometry as shown in Fig. 1. The longitudinal resistivity, ρ_{xx}, was measured. The applied current density in the resistivity measurement was $\sim 1\times 10^4$ A/cm^2. The applied magnetic fields up to 5 T were parallel to the *c* axis and the *ab* plane of the film. We obtained the superconducting upper critical fields, $H_{c2,ab}$ and $H_{c2,c}$, the coherence lengths ξ_{ab} and ξ_c from the 50% resistive transition.

III. RESULTS AND DISCUSSION

A. Resistive transition

In Fig. 2 we show the resistivity as a function of temperature for YBCO/PBCO superlattices with varied thickness in magnetic fields of 0, 1, 2, 3, and 4 T parallel and perpendicular to the crystal *c* axis, respectively. The resistivity under magnetic field shows a broadening behavior. The broadening

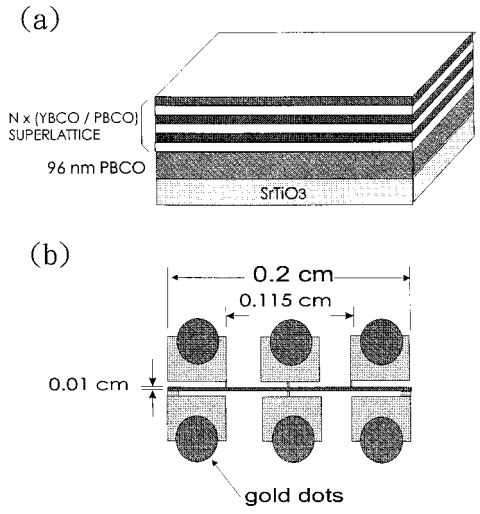

FIG. 1. (a) Schematics of a YBCO/PBCO layer structure buffered with 96 nm PBCO layer and (b) the resistivity and Hall pattern of a YBCO/PBCO superlattice.

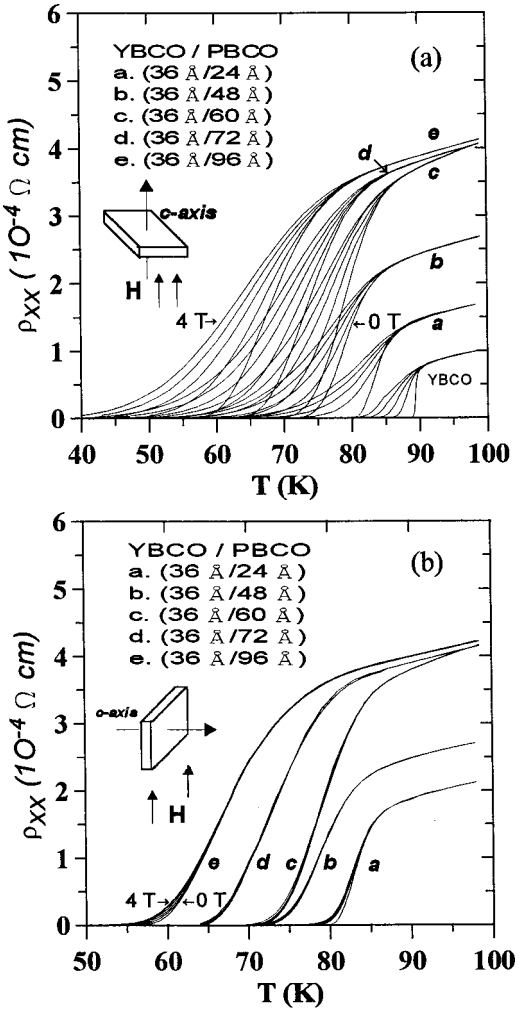

FIG. 2. Resistivities as a function of temperature for YBCO/PBCO superlattices with applied magnetic fields parallel to (a) the *c* axis (b) the *ab* plane. The applied magnetic fields were 0, 1, 2, 3, and 4 T.

is wider in fields parallel to the *c* axis compared with the data obtained with fields parallel to the *ab* plane. The results demonstrate the anisotropic properties of superlattices and are similar to that observed by other groups in thin films and superlattices.[1,3]

B. Anisotropy upper critical fields $H_{c2,c}(T)$ and $H_{c2,ab}(T)$

In Fig. 3 we show the upper critical fields $H_{c2,c}(T)$ and $H_{c2,ab}(T)$ as a function of temperature for a series of (YBCO/PBCO) superlattices. The $H_{c2,c}(T)$ and $H_{c2,ab}(T)$ show a linear behavior. The values of $-dH_{c2,c}(T)/dT$ and $-dH_{c2,ab}(T)/dT$ along with other series of YBCO/PBCO superlattices are shown in Table I. The values of $H_{c2,c}(0)$ and $H_{c2,ab}(0)$ are derived using the formula derived by Werthamer, Helfand, and Hohenberg:[8] $H_{c2}(0) = 0.693 T_c \lvert dH_{c2}(T)/dT \rvert_{Tc}$. For the series of $(120\,\text{Å}/48\,\text{Å})_8$, $(96\,\text{Å}/48\,\text{Å})_{10}$, $(60\,\text{Å}/48\,\text{Å})_{16}$, $(48\,\text{Å}/48\,\text{Å})_{20}$, and $(36\,\text{Å}/48\,\text{Å})_{26}$ superlattices, the values of $H_{c2,c}(0)$ varied from (71.67 ± 6.07) to (47.49 ± 1.66) T in magnetic field parallel to the crystal *c* axis while the $H_{c2,ab}(0)$ varied from (509.21 ± 21.9) to (1458.5 ± 87.26) T in magnetic field parallel to the crystal *ab* plane. The value of $-dH_{c2,c}(T)/dT$ varied from (1.18 ± 0.1) T/K to (0.86 ± 0.03) T/K in a magnetic field parallel to the crystal *c* axis and varied from (8.39 ± 0.36) T/K to (26.41 ± 1.58) T/K in a magnetic field parallel to the crystal *ab* plane for $(120\,\text{Å}/48\,\text{Å})_8$, $(96\,\text{Å}/48\,\text{Å})_{10}$, $(60\,\text{Å}/48\,\text{Å})_{16}$, $(48\,\text{Å}/48\,\text{Å})_{20}$, and $(36\,\text{Å}/48\,\text{Å})_{26}$ superlattices.

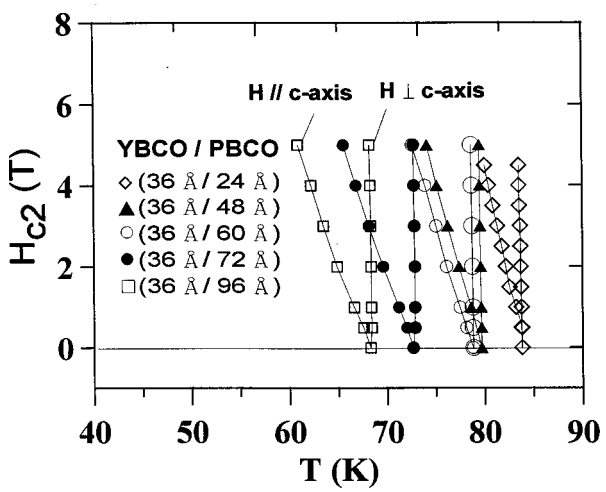

FIG. 3. Upper critical fields $H_{c2,c}(T)$ and $H_{c2,ab}(T)$ as a function of temperature for (YBCO/PBCO) superlattices with applied magnetic fields parallel to the *c* axis and the *ab* plane.

C. Coherence lengths ξ_{ab} and ξ_c

For isotropic superconducting materials the coherence length, ξ, can be obtained from the Ginzburg-Landau (GL) theory and ξ is given by the formula $\xi = (\Phi_0/2\pi H_{c2})^{1/2}$, where $\Phi_0 = hc/2e$ is the flux quantum and H_{c2} is the upper critical field. For anisotropic superconductors, the GL theory has been extended to include the anisotropic properties. The coherence lengths, ξ_{ab} and ξ_c, in the anisotropic GL theory are related to the upper critical fields $H_{c2,c}$ and $H_{c2,ab}$ by the formulas

$$\xi_{ab} = (\Phi_0/2\pi H_{c2,c})^{1/2}, \tag{1}$$

$$\xi_c = \Phi_0/2\pi H_{c2,ab}\xi_{ab}, \tag{2}$$

where $H_{c2,c}$ is the upper critical field with the applied magnetic field parallel to the *c* axis, $H_{c2,ab}$ is upper critical field with the applied magnetic field parallel to the *ab* plane. We derived the superconducting upper critical fields, $H_{c2,ab}$ and $H_{c2,c}$, the coherence lengths ξ_{ab} and ξ_c from the 50% resistive transition. Table II shows the obtained values of $\xi_{ab}(0)$ and $\xi_c(0)$ along with the anisotropy ratio, $\gamma = (\xi_{ab}/\xi_c)$, for a series of YBCO/PBCO superlattices. The values of $\xi_{ab}(0)$ and $\xi_c(0)$ for YBCO films are 20.2 Å and 3.1 Å, respectively, which are close to the reported values[9] of 16–24 Å for $\xi_{ab}(0)$ and 3–7 Å for $\xi_c(0)$. Typical high-T_c superconductors are $YBa_2Cu_3O_y$ with anisotropy ratio $\gamma = 5-8$,[10,11] $Bi_2Sr_2CaCu_2O_y$ (BSCCO) with $\gamma = 55-150$,[12,13] and $Tl_2Ba_2CaCu_2O_y$ with $\gamma = 70-350$.[14,15] For YBCO/PBCO superlattices with a fixed thickness of PBCO layer and a decreased thickness of YBCO layers, the value of $\xi_{ab}(0)$ increases while the value of $\xi_c(0)$ decreases. However, for YBCO/PBCO superlattices with a fixed thickness of the

TABLE I. Upper critical fields and $[dH_{c2}/dT]_{T_c}$ parameters for a series of YBCO/PBCO superlattices with a fixed PBCO thickness. The subscript n of each sample refers to the number of modulation layer of YBCO/PBCO superlattices. For example, this (120 Å/48 Å)$_8$ sample has 8 modulation layers.

Samples (YBCO/PBCO)	$H_{c.2c}(0)$ (T)	$H_{c2,ab}(0)$ (T)	$-[dH_{c2,c}/dT]_{T_c}$ (T/K)	$-[dH_{c2,ab}/dT]_{T_c}$ (T/K)
YBCO	80.80±6.84	524.59±13.05	1.30±0.11	8.44±0.21
(120 Å/48 Å)$_8$	71.67±6.07	509.21±21.85	1.18±0.10	8.39±0.36
(96 Å/48 Å)$_{10}$	67.50±6.63	546.05±79.56	1.12±0.11	9.06±1.32
(60 Å/48 Å)$_{16}$	62.20±7.04	755.75±68.06	1.06±0.12	12.88±1.16
(48 Å/48 Å)$_{20}$	54.95±2.83	1165.35±196.02	0.97±0.05	20.57±3.46
(36 Å/48 Å)$_{26}$	47.49±1.66	1458.50±87.26	0.86±0.03	26.41±1.58
(96 Å/60 Å)$_{10}$	68.4 ±1.78	525.21±29.74	1.15±0.03	8.83±0.50
(60 Å/60 Å)$_{16}$	65.85±2.91	715.03±125.29	1.13±0.05	12.27±2.15
(48 Å/60 Å)$_{20}$	45.42±3.36	1281.77±264.09	0.81±0.06	22.86±4.71
(36 Å/60 Å)$_{26}$	44.25±1.64	1532.35±1.64	0.8 ±0.03	28.05±0.03
(60 Å/24 Å)$_{10}$	80.39±4.84	509.54±139.02	1.33±0.08	8.43±2.30
(48 Å/24 Å)$_{20}$	58.50±2.36	725.65±166.04	0.99±0.04	12.28±2.81
(36 Å/24 Å)$_{26}$	55.75±3.48	870.04±131.26	0.96±0.06	14.98±2.26
(120 Å/96 Å)$_8$	71.79±4.79	607.84±70.60	1.20±0.08	10.16±1.18
(48 Å/96 Å)$_{20}$	59.94±2.20	1214.72±332.69	1.09±0.04	22.09±6.05
(36 Å/96 Å)$_{26}$	31.41±2.38	1314.58±300.80	0.66±0.05	27.62±6.32

YBCO layers and a decreased thickness of PBCO layers, the value of $\xi_{ab}(0)$ decreases while the value of $\xi_c(0)$ increases. All superlattices showed satellite peaks in the powder x-ray diffraction pattern and the surface probed by the atomic surface microscope (AFM) revealed smooth morphology in YBCO/PBCO superlattices as reported in Ref. 7. The x-ray and AFM data confirmed that the YBCO layers of different thickness are of the same high quality. We noted in Table II the coherence length $\xi_{ab}(0)$, of (120 Å/48 Å), (96 Å/48 Å), (60 Å/48 Å), (48 Å/48 Å), and (36 Å/48 Å) superlattices, increases monotonically from (21.5 ± 0.9) Å to (26.3 ± 0.5) Å while the coherence length, $\xi_c(0)$, decreases systematically from (3.1 ± 0.2) Å to (0.9 ± 0.1) Å.

TABLE II. Parameters of $\xi_{ab}(0)$, $\xi_c(0)$, and $\gamma=(\xi_{ab}/\xi_c)$ for a series of YBCO/PBCO superlattices with a fixed PBCO thickness. The subscript of each sample refers to the number of modulation layers of YBCO/PBCO superlattices. For example, the (120 Å/48 Å)$_8$ sample has 8 modulation layers.

Samples (YBCO/PBCO)	$\xi_{ab}(0)$ (Å)	$\xi_c(0)$ (Å)	γ
YBCO	20.2±0.9	3.1±0.2	6.5
(120 Å/48 Å)$_8$	21.5±0.9	3.0±0.3	7.1
(96 Å/48 Å)$_{10}$	22.1±1.1	2.7±0.5	8.2
(60 Å/48 Å)$_{16}$	23.0±1.3	1.9±0.3	12.1
(48 Å/48 Å)$_{20}$	24.5±0.6	1.2±0.2	20.4
(36 Å/48 Å)$_{268}$	26.3±0.5	0.9±0.1	29.2
(96 Å/60 Å)$_{10}$	22.0±0.3	2.9±0.2	7.6
(60 Å/60 Å)$_{16}$	22.4±0.5	2.1±0.4	10.7
(48 Å/60 Å)$_{20}$	26.9±0.1	1.0±0.2	26.9
(36 Å/60 Å)$_{26}$	27.9±0.5	0.8±0.02	34.9
(60 Å/24 Å)$_{10}$	20.2±0.6	3.2±1.0	6.3
(48 Å/24 Å)$_{20}$	23.7±0.5	1.9±0.5	12.5
(36 Å/24 Å)$_{26}$	24.3±0.8	1.6±0.3	15.2
(120 Å/96 Å)$_8$	21.4±0.7	2.5±0.4	8.6
(48 Å/96 Å)$_{20}$	23.4±0.4	1.2±0.3	19.5
(36 Å/96 Å)$_{26}$	32.4±1.2	0.8±0.2	40.5

Terashima *et al.*[16] reported one-unit-cell thick of YBCO layer sandwiched between PBCO layers (6 PBCO layers). They observed a broad superconconducting transition [$T_{c,\text{zero}}\sim20$ K and $T_c(50\%)\sim50$ K]. The unit cell thickness of YBCO layer is ~12 Å along the c axis. Both (YBCO/PBCO) (120 Å/48 Å) and (YBCO/PBCO) (36 Å/48 Å) superlattices have the same thickness of individual PBCO layers (48 Å thick). Nevertheless, the (YBCO/PBCO) (120 Å/48 Å) superlattice shows $T_{c,\text{zero}}(50\%)$ at 87.6 K while the (YBCO/PBCO) (36 Å/48 Å) superlattice shows $T_{c,\text{zero}}(50\%)$ at 79.7 K. From the T_c data of Terashima *et al.* and the T_c data of the (120 Å/48 Å) and (36 Å/48 Å) superlattices we conclude that (1) there exists an one-unit-cell YBCO coupling both in the 120 Å thick (ten-units-cell of YBCO layer) YBCO layer and 36 Å thick (three-units-cell of YBCO layer) YBCO layers and (2) the one-unit-cell YBCO coupling in the 120 Å thick YBCO layers is stronger than that of the 36 Å thick YBCO layer. It is noted a single layer of YBCO film (120 Å thick) shows $T_c(50\%)\sim80$ K while the (YBCO/PBCO) (120 Å/48 Å) superlattice shows $T_{c,\text{zero}}(50\%)$ at 87.6 K. Therefore, besides the one-unit-cell YBCO coupling, there exists also an interlayer coupling between the YBCO layers in YBCO/PBCO (120 Å/48 Å) superlattice. Decreasing the distance between YBCO layers and adding one unit cells to individual YBCO layer leads to an increased critical temperature, that closer unit cells either adjacent or separated by PBCO layers implies stronger coupling, that such cou-

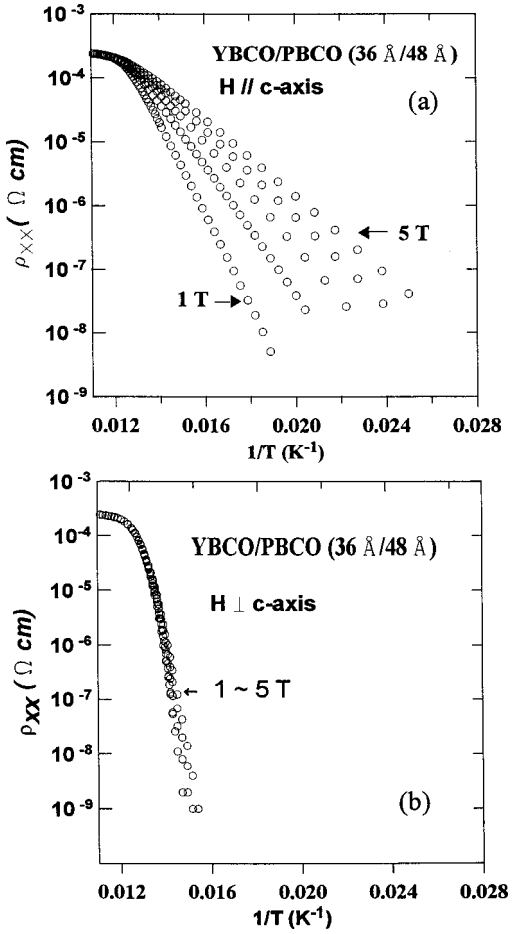

FIG. 4. $\log \rho_{xx}$ versus $1/T$ plot for a YBCO/PBCO (36 Å/48 Å) superlattice under applied magnetic fields parallel to (a) the *c* axis and (b) the *ab* plane.

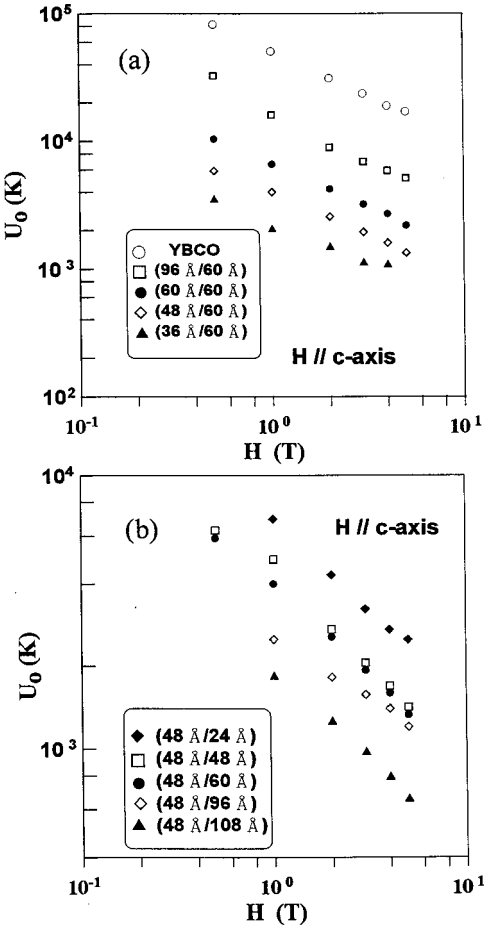

FIG. 5. Activation energy as a function of magnetic field for different superlattices.

pling is expected to raise T_c. Due to both the stronger interlayer and one-unit-cell couplings in (YBCO/PBCO) (120 Å/48 Å) superlattice, therefore, a longer $\xi_c(0)$ was observed in the YBCO/PBCO (120 Å/48 Å) superlattice compared with that of the YBCO/PBCO (36 Å/48 Å) superlattice.

D. The activation energy $U(T,H)$

It has been found that the lower part of the resistive transition under magnetic fields can be described by the formula[3]

$$\rho(T,H)=\rho_0 \exp[-U_0(T,H)/k_BT], \tag{3}$$

where U_0 is the activation energy which depends on temperature and the applied field H, ρ_0 is the prefactor of the resistivity. This behavior is generally understood as a thermally activated flux motion. This thermally activated mechanism of flux motion was proposed by Anderson[17] and later by Anderson and Kim.[18]

As shown in Fig. 4 the thermally activated behavior is evident in $\log \rho_{xx}$ versus $1/T$ plot for a YBCO/PBCO (36 Å/48 Å) superlattice. The straight lines in the $\log \rho_{xx}$ versus $1/T$ plot for low resistivity indicate that the dissipation mechanism is thermally activated flux flow, and the slopes give the activation energy U_0. For all samples the U_0 can be fitted to the field-dependence $U_0 \sim H^{-\alpha}$ with α in the ranges of 0.44–0.79 as shown in Fig. 5.

Regarding the flux pinning energy $U_0(T)$, Yeshrum and Melozemoff[19] by a scaling argument suggested that the activation energy:

$$U_0 = f \times (\mu_0 H_c^2/2) V_c, \tag{4}$$

where f is the fraction of the condensation energy, H_c is the thermodynamic critical field, V_c is the volume of flux involved in the activation process. $V_c = R_c^2 L_c$ with correlation lengths R_c and L_c. The R_c and the L_c give the size of the correlated region of the vortex perpendicular and parallel to the magnetic field, respectively. Taking R_c as the average distance between the flux lines, i.e., $R_c \sim 1.075(\phi_0/H)^{1/2}$.[19] Equation (4) therefore can be rewritten as

$$U_0 \sim f \times (\mu_0 H_c^2/2)(\Phi_0/H) \times L_c. \tag{5}$$

Some experimental data showed that U_0 is proportional to $(1/H^{\alpha})$ with $\alpha = 0.76$–0.88, deviating a little from $\alpha = 1$ that is expected from Eq. (5) in epitaxial $YBa_2Cu_3O_y$ films,[20] while other experimental results showed that the power law magnetic field dependence, $U_0 \sim (1/H^{\alpha})$, $\alpha = 0.25$–0.5 for $Bi_2Sr_2CaCu_2O_8$,[3] deviating a lot from $\alpha = 1$. For all superlattice samples the U_0 can be fitted to the field-dependence $U_0 \sim H^{-\alpha}$ with α in the range of 0.44–0.79. Equation (5) which shows that U_0 is inversely proportional H, is not consistent with the observed power law dependence of U_0 in superlattices.

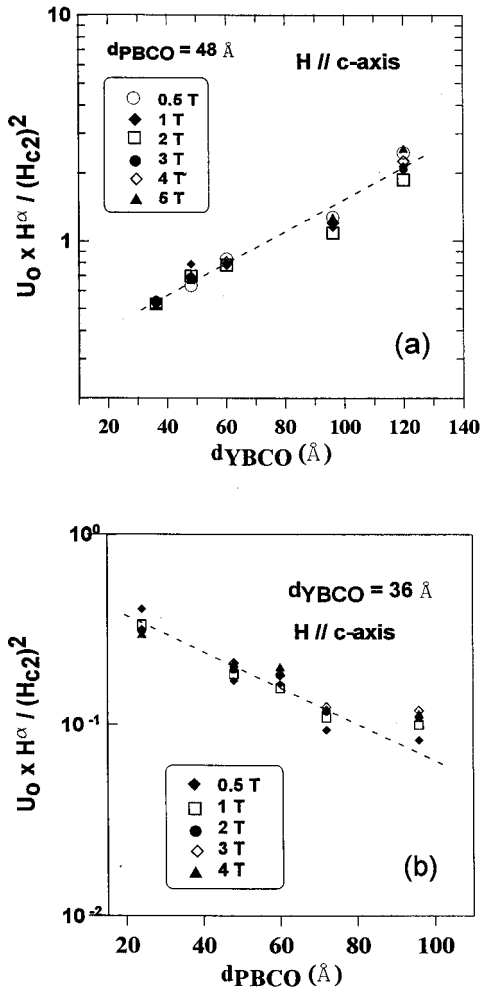

FIG. 6. The $U_0H^\alpha/(H_{c2,c})^2$ as a function of layer thickness for YBCO/PBCO superlattices (a) with a fixed thickness of PBCO layer (48 Å thick) and varied thickness of YBCO layer and (b) with a fixed thickness of YBCO layer (36 Å thick) and varied thickness of PBCO layer, where U_0 is the pinning energy, α is the magnetic field exponent, and $H_{c2,c}$ is the upper critical field with the applied field parallel to the c axis.

Figure 6(a) shows $U_0\times H^\alpha/(H_{c2,c})^2$ as a function of layer thickness for YBCO/PBCO superlattices with a fixed thickness of PBCO layer (48 Å thick) and varied thickness of YBCO layer under magnetic fields parallel to the c axis while Fig. 6(b) shows the $U_0\times H^\alpha/(H_{c2,c})^2$ as a function of layer thickness for YBCO/PBCO superlattices with a fixed thickness of YBCO layer (36 Å thick) and varied thickness of PBCO layer under varied magnetic fields, where U_0 is the pinning energy, α is the magnetic field exponent, and $H_{c2,c}$ is the upper critical field with the applied field parallel to the c axis. Several features were observed in Fig. 6. First, $U_0\times H^\alpha/(H_{c2,c})^2$ was found to fall at the same value for different magnetic fields in $(YBCO/PBCO)_n$ superlattices with different thickness of YBCO [Fig. 6(a)] or PBCO [Fig. 6(b)] layers; second $\log[U_0\times H^\alpha/(H_{c2,c})^2]$ increases linearly as the thickness of YBCO layers is increased [Fig. 6(a)] and $\log[U_0\times H^\alpha/(H_{c2,c})^2]$ decreases linearly as the thickness of the PBCO layers is increased [Fig. 6(b)].

For a fixed thickness of PBCO layer (48 Å thick) and an increased thickness of YBCO layers, the coupling of YBCO layers is stronger, we have observed an increased value of $U_0H^\alpha/(H_{c2,c})^2$ [Fig. 6(a)]. For a fixed thickness of YBCO layer (36 Å) and an increased thickness of the PBCO layer, there is a decoupling of YBCO layers and we have observed a decreased value of $U_0H^\alpha/(H_{c2,c})^2$ [Fig. 6(b)]. All superlattices reported here have a total thickness of 960 Å in YBCO layers. From the results shown in Fig. 6 we draw the following conclusions: (1) the U_0 scales to $(H_{c2,c})^2/H^\alpha$ under different magnetic fields in $(YBCO/PBCO)_n$ superlattices with different thickness of YBCO and PBCO layers, (2) the U_0 depends on the coupling strengths of YBCO layers, its value is larger when the coupling strength of the YBCO layers is increased and decreases when there is decoupling in the YBCO layers.

IV. CONCLUSION

The resistivity of $(YBCO/PBCO)_n$ superlattices under magnetic fields can be described by the thermally activated flux-flow resistivity: $\rho(T,H)=\rho_0\exp[-U_0(T,H)/k_BT]$. A power law magnetic field dependence of $U_0\sim H^{-\alpha}$ in YBCO/PBCO superlattices was observed. The quantity $\log[U_0\times H^\alpha/(H_{c2,c})^2]$ was observed to be a constant for a given sample but increased linearly as the thickness of YBCO layers increased and decreases linearly as the thickness of the PBCO layers increased. There exists one-unit-cell YBCO and interlayer YBCO couplings in YBCO/PBCO superlattices. These couplings affect the coherence lengths

ACKNOWLEDGMENT

The authors thanks the National Science Council of the Republic of China for financial support under Grant No. NSC88-2112-M002-020.

[1] T. T. M. Palstra, B. Batlogg, L. F. Schneemeyer, and J. V. Waszcak, Phys. Rev. Lett. **61**, 1662 (1988).

[2] P. H. Kes, J. Aart, J. van den Berg, C. J. van der Beek, and J. A. Mydosh, Supercond. Sci. Technol. **1**, 242 (1989).

[3] T. T. M. Palstra, B. Batlogg, R. B. van Dover, L. F. Schneemeyer, and J. V. Wasczak, Phys. Rev. B **41**, 6621 (1990).

[4] M. V. Feigelman, V. B. Geshkenbien, and A. I. Larkin, Physica C **167**, 177 (1990).

[5] O. Brunner, L. Antognazza, J.-M Triscone, L. Miéville, and Ø. Fisher, Phys. Rev. Lett. **67**, 1354 (1991); L. Antognazza, O. Brunner, L. Miéville, J.-M. Triscone, and Ø. Fisher, Physica C **185-189**, 2081 (1991).

[6] L. M. Wang, H. W. Yu, H. C. Yang, and H. E. Horng, Physica C **256**, 57 (1996).

[7] H. C. Yang, L. M. Wang, and H. E. Horng, Physica C **281**, 325 (1997).

[8] N. R. Werthermer, E. Helfand, and P. C. Hohenberg, Phys. Rev. B **48**, 6703 (1993).

[9] U. Welp, W. K. Kwok, G. W. Crabtree, K. G. Vandervoot, and J. Z. Liu, Phys. Rev. Lett. **62**, 1908 (1989).

[10] D. E. Farallel, C. M. Williams, S. A. Wolf, N. P. Bansal, and V. G. Kogan, Phys. Rev. Lett. **61**, 2805 (1988).
[11] D. E. Farallel, J. P. Rice, D. M. Ginsberg, and J. Z. Liu, Phys. Rev. Lett. **64**, 1573 (1990).
[12] D. E. Farallel, S. Bonham, J. Foster, Y. C. Chang, P. Z. Jiang, K. G. Vandervoort, D. J. Lam, and V. G. Kogan, Phys. Rev. Lett. **63**, 782 (1989).
[13] J. C. Martinez, S. H. Brongersma, A. Koshelev, B. Ivlev, P. H. Kes, R. P. Griessen, D. G. de Groot, Z. Tarnavski, and Menovsky, Phys. Rev. Lett. **69**, 2276 (1992).
[14] K. E. Gray, R. T. Kampwirth, and D. E. Farrel, Phys. Rev. B **41**, 819 (1990).
[15] D. E. Farallel, R. G. Beck, M. F. Booth, C. J. Bukowski, and D. M. Ginsberg, Phys. Rev. B **42**, 6758 (1990).
[16] T. Terashima, K. Shimura, and Y. Bando, Y. Matsuda, A. Fujiyama, and S. Komiyama, Phys. Rev. Lett. **67**, 1362 (1991).
[17] P. W. Anderson, Phys. Rev. Lett. **9**, 309 (1962).
[18] P. W. Anderson and Y. B. Kim, Rev. Mod. Phys. **36**, 39 (1964).
[19] Y. Yeshurun and A. P. Malozemoff, Phys. Rev. Lett. **60**, 2202 (1988).
[20] E. Zeldov, N. M. Amer, G. Koren, A. Gupta, R. J. Gambino, and M. W. McElfresh, Phys. Rev. Lett. **62**, 3093 (1989).